Geochemical Perspectives Letters EAG

Residual forearc peridotites recording the early magmatic stage of subduction initiation

I. Nishio[1,2*], N. Akizawa[1], T. Ishii[3], K. Itano[4], A. Tamura[5], T. Morishita[5,6]

OPEN ACCESS
https://doi.org/10.7185/geochemlet.2624

Abstract

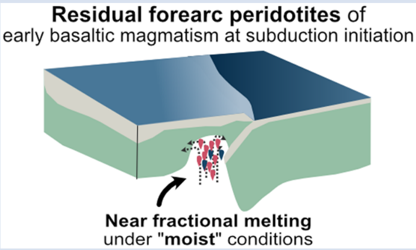

Subduction initiation is fundamental to plate tectonics. Early basaltic magmatism preceding boninitic magmatism is key to understanding the onset and mechanism of subduction initiation. However, the mantle processes during the early basaltic magmatism remain poorly understood due to the scarcity of corresponding residual peridotites. To find the residual peridotites from the early stage of subduction initiation, we compiled spinel data and examined peridotites from the Izu-Bonin-Mariana and Tonga forearc regions that contain some of the lowest spinel Cr/Al ratios. These samples present small amounts of pargasitic amphibole and light rare earth elements depleted patterns in their clinopyroxenes and amphiboles. These features differ from depleted forearc peridotites associated with boninitic magma, abyssal peridotites, and backarc peridotites, but resemble lherzolites from the Oman ophiolite. Melting models can reproduce the compositions of clinopyroxene and the corresponding early basalts for each region. We suggest that the studied forearc peridotite samples are residues after early basaltic magma extractions, which potentially involved a common process of near fractional melting under moist conditions.

Received 12 January 2026 | Accepted 18 May 2026 | Published 30 June 2026

Introduction

Subduction initiation is a crucial process for the onset of plate tectonics and arises from a complex interplay between internal and external plate forces, plate structure, and physicochemical properties of the mantle (Stern and Gerya, 2018; Maunder *et al.*, 2020). Izu-Bonin-Mariana (IBM) and Tonga forearc regions in the western Pacific are the "modern" analogues (Fig. S-1), where tectonic configurations have been constrained by the studies on magmatic rocks and geophysical observation. Subduction initiation occurred around 50 Ma in both regions (Crameri *et al.*, 2020). In the IBM region, the Pacific Plate started to subduct beneath the Proto-Philippine Sea Plate along a pre-existing fracture zone (Ishizuka *et al.*, 2011). Following the onset of subduction initiation, the slab sinking induced a counter asthenospheric mantle flow, which drove seafloor spreading and generated an early mid-ocean ridge basalt (MORB)-like basalt, known as forearc basalt (FAB) (Reagan *et al.*, 2010). As the slab descended further, it released fluids that triggered melting of the residual mantle *via* slab-derived fluid influx, which in turn resulted in boninitic magmatism (Ishizuka *et al.*, 2020). In the Tonga region, subduction initiation occurred when the Pacific plate started to subduct beneath the Australian plate (Crameri *et al.*, 2020). This was triggered by the collision of the Papuan peninsula with the trench of the New Caledonia subduction zone (Meffre *et al.*, 2012). The basalt in the Tonga region, interpreted as a product of subduction initiation, is known as early arc tholeiite (EAT) (Todd *et al.*, 2012). The early basaltic magmatism, which can provide the earliest record of subduction initiation, is the key to understanding subduction initiation mechanism.

Forearc peridotites are expected to record the magmatic evolution associated with the subduction initiation (*e.g.*, Birner *et al.*, 2017). Recovered forearc peridotites are mostly depleted, associated with boninitic magmatism, characterised by high spinel Cr# [= Cr/(Cr + Al)] ($>\sim 0.6$; Fig. 1) (*e.g.*, Loocke and Snow, 2024). Rarely, forearc peridotites with low spinel Cr# experienced reaction with early basaltic melts have been reported (Morishita *et al.*, 2011; Birner *et al.*, 2017). However, the residual forearc peridotites that retain the information of early basaltic magma extraction have not yet been identified. This is most likely because the signatures of the early basaltic magmatism were overprinted by subsequent melt-rock reaction, boninitic magmatism, and later geological processes. Such residual peridotites are the crucial piece for constraining the mantle processes corresponding to the early stage of subduction initiation. We systematically examined spinel data from forearc peridotites to evaluate their compositional variation and re-investigated forearc peridotite samples with among the lowest spinel Cr# from the IBM and Tonga regions.

1. Graduate School of Advanced Science and Engineering, Hiroshima University, Hiroshima 739-8526, Japan
2. Department of Geosciences and Natural Resource Management, University of Copenhagen, Copenhagen 1350, Denmark
3. Center for Integrated Research and Education of Natural Hazards, Shizuoka University, Shizuoka 422-8529, Japan
4. Submarine Resources Research Program, Institute for Earth and Material Sciences, Japan Agency for Marine-Earth Science and Technology, Kanagawa 237-0061, Japan
5. School of Geosciences and Civil Engineering, Kanazawa University, Kanazawa 920-1192, Japan
6. Volcanoes and Earth's Interior Research Center, Research Institute for Marine Geodynamics, Japan Agency for Marine-Earth Science and Technology, Kanagawa 237-0061, Japan
* Corresponding author (email: iknishio@hiroshima-u.ac.jp)

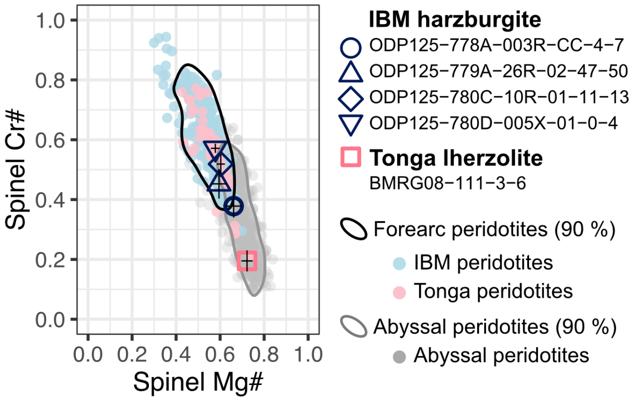

Figure 1 Spinel Cr# [= Cr/(Cr + Al)] *vs.* Mg# = [Mg/(Mg + Fe)] plot. The areas represent the 90 % density contours for spinels from abyssal and forearc peridotites, respectively. Abyssal spinel data are from Warren (2016). References for spinel data from the IBM and Tonga forearc peridotites are listed in the Supplementary Information.

Results

Morishita *et al.* (2011) and Birner *et al.* (2017) identified peridotites with low spinel Cr# that record reactions with early basalts (~0.5 for IBM and 0.3 for Tonga, respectively). Because melt-rock reactions generally increase spinel Cr# (Pearce *et al.*, 2000), residual peridotites that experienced only partial melting and basaltic melt extraction are expected to have lower spinel Cr#. Such samples (Cr# < 0.4) account only for ~4 % of forearc spinel data but do occur (Fig. 1). Based on the Cr# thresholds (~0.5 for IBM and 0.3 for Tonga), we investigated five samples with low spinel Cr# (four from IBM and one from Tonga) (Figs. S-2, S-3). The samples from the IBM region were collected from Conical seamount during ODP Leg 125 (Ishii *et al.*, 1992). IBM harzburgite sample (ODP125-778A-003R-CC-4–7) has spinel Cr# (0.38 ± 0.03, average ± 2σ) at the low end of the forearc peridotite field (Fig. 1). The other three samples show spinel Cr# (average 0.45, 0.52, and 0.57), which are more similar to the Cr# threshold for IBM (~0.5) (Morishita *et al.*, 2011). For the Tonga region, we were able to investigate a lherzolite sample (BMRG08-111-3-6) with the lowest spinel Cr# (0.19 ± 0.03; Fig. 1) well below the threshold (0.3) for Tonga (Birner *et al.*, 2017). This sample was collected during the 1996 Boomerang Leg 8 cruise from the northern part of the Tonga forearc.

Rare earth elements (REEs) in clinopyroxenes from the lowest Cr# spinel-bearing IBM harzburgite and the Tonga lherzolite are characterised by light REE (LREE) depleted patterns with relatively high heavy REE (HREE) contents (Fig. 2). In the IBM harzburgite, LREE contents in clinopyroxenes are lower than detection limits, *i.e.* LREE depleted. The LREE depleted patterns of clinopyroxenes from these samples contrast with those from depleted forearc peridotites, which display high LREE/HREE ratios and low HREE contents (Day and Brown, 2021; Loocke and Snow, 2024). Clinopyroxenes from the IBM harzburgite show comparable REE contents to those from the LREE depleted residual abyssal peridotites formed after extensive partial melting and melt extraction. Clinopyroxenes from the Tonga lherzolite show similar REE patterns to those from general abyssal peridotites (Warren, 2016). Clinopyroxenes from the IBM samples with slightly higher spinel Cr# (>0.45) show lower HREE contents with detectable contents of LREE, which share the characteristics of depleted forearc peridotites.

Pargasitic amphiboles (<0.1 vol. %), are observed in the IBM harzburgite and the Tonga lherzolite with the lowest Cr#, where they are surrounded by orthopyroxene and/or adjacent to clinopyroxene (Fig. 3a,b). Amphiboles are often found in forearc and backarc peridotites (Morishita *et al.*, 2011; Akizawa *et al.*, 2021) but are rare in abyssal peridotites (Cipriani *et al.*, 2009). Amphiboles also occur in basal lherzolites with low spinel Cr# (~0.2) of the supra-subduction zone Oman ophiolite (Prigent *et al.*, 2018). Pargasitic amphiboles show relatively high TiO_2 (IBM, 0.45 wt. %; Tonga, 0.75 wt. %) and low K_2O contents (<~0.1 wt. %) (Fig. 3c), which resemble those from abyssal peridotites and from Oman basal lherzolites. Amphiboles from

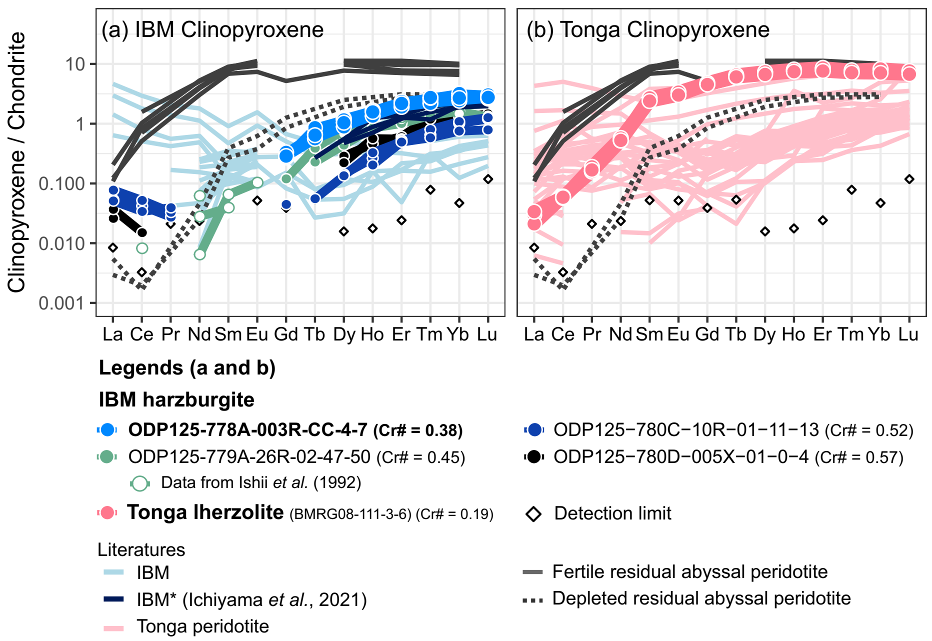

Figure 2 Chondrite normalised REE patterns of clinopyroxene from **(a)** the IBM forearc peridotites and **(b)** the Tonga forearc peridotites. Cr# indicates the value of the coexisting spinel. References for clinopyroxene data of IBM peridotites, Tonga peridotites, and fertile and depleted abyssal peridotites are listed in the SI.

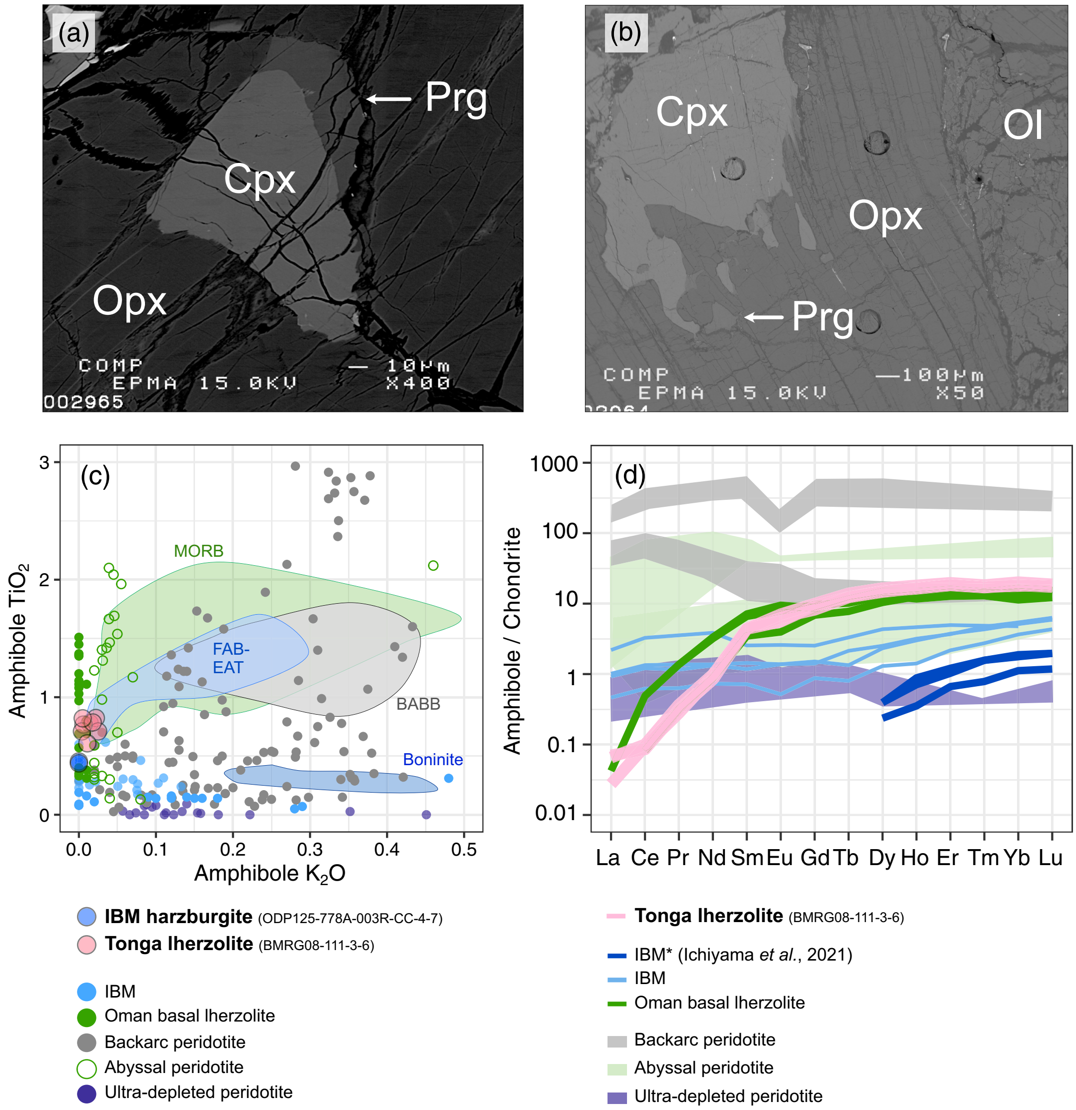

Figure 3 Back scatter electron images of **(a)** the IBM harzburgite (ODP125-778A-003R-CC-4–7) and **(b)** the Tonga lherzolite (BMRG08-111-3-6). Ol, olivine; Opx, orthopyroxene; Cpx, clinopyroxene; and Prg, pargasite. **(c)** TiO_2-K_2O discrimination plot and **(d)** chondrite normalised REE patterns for amphibole from the IBM harzburgite and the Tonga lherzolite, compared with data from forearc, ultra-depleted, backarc, and abyssal peridotites, as well as Oman basal lherzolites. Areas for mid-ocean ridge basalt (MORB), backarc basin basalt (BABB), forearc basalt and early arc tholeiite (FAB-EAT), and boninite are shown in **(c)**. References for amphibole data are provided in the SI.

backarc and depleted forearc peridotites show distinct compositions: backarc amphiboles display variable and higher TiO_2 and K_2O contents, whereas amphiboles from depleted peridotites are characterised by low TiO_2 and high K_2O contents.

Pargasitic amphiboles in the Tonga lherzolite show LREE depleted patterns similar to those of the coexisting clinopyroxenes, and to amphiboles from Oman basal lherzolites (Fig. 3d). We could not analyse trace element compositions of pargasite in the IBM harzburgite due to its small grain size. Notably, amphiboles and clinopyroxenes from one IBM sample exhibit LREE contents below detection limits (Figs. 2a, 3d; Ichiyama *et al.*, 2021). Such LREE depleted patterns differ from those of backarc peridotites (Gong *et al.*, 2022), abyssal peridotites (Cipriani *et al.*, 2009), depleted peridotites in relation to boninitic magmas (Nishio *et al.*, 2023), and IBM dunites formed by reaction with FAB (Morishita *et al.*, 2011).

Sample information, analytical methods, and mineral major and trace element compositions are provided in the SI and SI Tables.

Discussion

IBM harzburgite ODP125-778A-003R-CC-4–7 and Tonga lherzolite BMRG08-111-3-6 are characterised by clinopyroxenes with LREE depleted patterns and relatively high HREE contents, and low spinel Cr# (Figs. 1, 2). These characteristics align them with residual abyssal peridotites that experienced partial melting and basaltic melt extraction without significant melt-rock reaction (Warren, 2016). Clinopyroxenes from the IBM samples with slightly high spinel Cr# (0.45, 0.52, and 0.57) show lower HREE and detectable LREE contents. Reactions with melts or fluids generally increase LREE contents in residues (Birner *et al.*, 2017). In our compiled forearc spinel data set ($n = 287$), 4 % of forearc peridotites exhibit low spinel Cr# (<0.4) and one IBM peridotite exhibits LREE depleted clinopyroxene patterns (Ichiyama *et al.*, 2021). The rare forearc peridotite samples with low spinel Cr# and LREE depleted clinopyroxene patterns represent potential mantle residues that preserve a record of partial melting during early basaltic magmatism of subduction initiation, without significant overprinting by melt-rock reactions.

Although the number of available samples is very limited and sampling bias cannot be ruled out, these samples nevertheless provide crucial direct evidence for early basaltic magmatism.

We therefore examined the samples (IBM, ODP125-778A-003R-CC-4–7; Tonga, BMRG08-111-3-6) to investigate melting processes and their link to early basaltic magmatism using an open system melting model (Ozawa, 2001). We conducted influx-free melting models using a depleted MORB mantle (DMM) source or a depleted DMM (DDMM) source (Workman and Hart, 2005). We varied two key parameters: the critical melt fraction (a_c: 0–2 %) at which melt starts to segregate, and the degree of melting (F: 0–25 %), with melting initiated in the garnet peridotite stability field (F_{grt}: 0–10 %) prior to the spinel peridotite stability fields. We compared the modelled clinopyroxene compositions ($n = \sim$20,000) with those of the studied samples corrected for subsolidus exchange, respectively (Figs. 4 and S-4–S-7). The modelled accumulated melt compositions were compared with FAB from the IBM region (Ishizuka *et al.*, 2011; Shervais *et al.*, 2019) and EAT from the Tonga region (Todd *et al.*, 2012), respectively.

Details of model set up, subsolidus correction, best fit model estimation, and model results are provided in the SI.

Our models show that REE contents in clinopyroxene decrease with increasing F. At a given F, increasing a_c suppresses LREE depletion, whereas increasing F_{grt} suppresses HREE depletion in clinopyroxene of spinel peridotite (Fig. S-5). At given F (>10 %), accumulated melt shows similar REE patterns regardless of a_c and F_{grt} (Fig. S-6). The modal Ce contents in accumulated melts are 2.98 ppm for models derived from the DDMM source and 3.86 ppm for those derived from the DMM source (Fig. S-7), reflecting slightly lower LREE contents in melts from the DDMM source.

Best fit models based on reduced chi square successfully reproduce the REE patterns of both clinopyroxene and basalt in each region (Figs. 4, S-8). For the IBM samples, the best fits correspond to $F = 16.8 \pm 2.1$ % (2σ) with $a_c = 0.4 \pm 0.6$ % and $F_{grt} = 2.9 \pm 3.8$ %. For the Tonga samples, the best fits correspond to $F = 7.4 \pm 0.1$ % with $a_c = 1$ % and $F_{grt} = 4$ %. Among IBM best fit models, 50.9 % adopt the DDMM source and 40.9 % the DMM source, whereas all Tonga best fit models are derived from the DMM source. Very low a_c (≤ 1 %) indicates that the melting conditions recorded in the studied forearc peridotites are near fractional melting, which is similar to the melting conditions beneath mid-ocean ridges (*e.g.*, Warren, 2016).

Given the similarity between the studied forearc peridotites and abyssal peridotites, there is a possibility that the studied samples might be remnants of abyssal peridotites that did not experience melting during subduction initiation. However, the studied samples contain minor amounts of pargasitic amphibole (Fig. 3) that are a common mineral phase in the forearc peridotites but not in the abyssal peridotites (Cipriani *et al.*, 2009; Morishita *et al.*, 2011). High TiO_2 and low K_2O contents in amphiboles from the studied samples support an origin related to early basalts (FAB and EAT) or MORB (Fig. 3c). LREE depleted patterns in amphiboles and clinopyroxenes from our studied samples and the IBM sample reported by Ichiyama *et al.* (2021) further contrast with those of amphiboles from abyssal peridotites, backarc peridotites, and ultra-depleted peridotites in relation to boninitic magmatism (Fig. 3d). Such LREE depleted clinopyroxenes and amphiboles have been reported from Oman basal lherzolites, where depleted harzburgites associated with boninites also occur (Prigent *et al.*, 2018). We therefore interpret the studied forearc peridotites as residues formed by partial melting and melt extraction during early basaltic magmatism at subduction initiation.

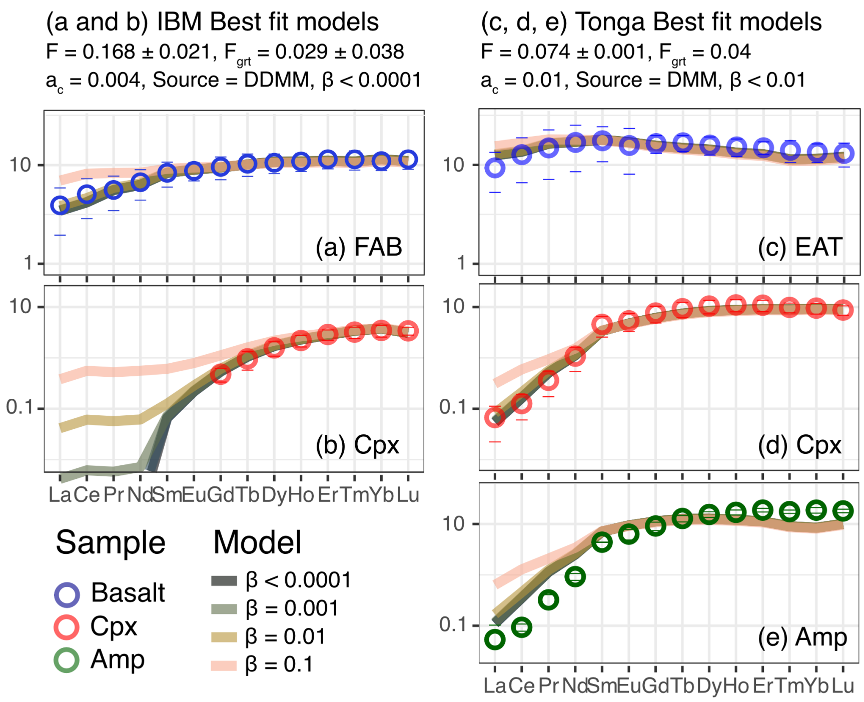

Figure 4 Chondrite normalised REE patterns: **(a,b)** IBM and **(c–e)** Tonga, showing **(a,c)** modelled accumulated melt compared with FAB and EAT, **(b,d)** modelled clinopyroxene compared with subsolidus-corrected clinopyroxene in IBM harzburgite ODP125-778A-003R-CC-4–7 and Tonga lherzolite BMRG08-111-3-6, and **(e)** modelled amphibole compared with amphiboles in the Tonga lherzolite. Sample symbols represent average values with ±2 standard deviations. All models are calculated at fixed melting degree (F), critical melt fraction (a_c), and source based on the best fit models (Fig. S-8), indicated at the top of each column, with colour denoting influx rate (β).

We further performed slab derived fluid (Li *et al.*, 2013; Shervais *et al.*, 2019) influx open system melting models to evaluate the effect of fluid infiltration and amphibole formation (Figs. 4 and S-9–S-11). Model settings are based on the best fit conditions constrained above, with the influx rate (β) varied from 0 to 1 and include amphibole crystallisation from a small fraction of trapped melt (0.1 %). At the best fit F (IBM, 16.8 %; Tonga, 7.4 %), increasing β suppresses LREE depletion in clinopyroxene (Fig. 4b,d), and amphibole shows similar REE behaviour (Fig. 4e). The effect of fluid infiltration on the accumulated melt is comparatively minor (Fig. 4a,c).

To reproduce the REE patterns of the studied clinopyroxene, β was required to be <0.0001 for the IBM samples to match LREE contents below detection limits, and <0.01 for the Tonga samples (Fig. 4b,d). These models simultaneously reproduced REE patterns of FAB and EAT, respectively (Fig. 4a,c), and capture the LREE depleted patterns of the Tonga amphibole (Fig. 4e). The very low a_c ($\leq$ 1 %) and β (<0.01), with the small trapped melt fraction (~0.1 %) also agree with the minor amounts of amphibole in the samples. Amphiboles in the studied samples may have formed during the early basaltic magmatic stage, through a combination of reactions with infiltrating fluids (Prigent *et al.*, 2018) at very low β, and crystallisation from a small fraction of trapped melts. Although the source of the fluid remains uncertain, our results imply that the melting conditions were not dry. "Moist" conditions have been proposed for the FAB formation based on their depleted REE patterns with slightly higher H_2O/Ce ratios compared to MORB (Brounce *et al.*, 2021), and lower TiO_2 contents at similar MgO contents relative to MORB (MacLeod *et al.*, 2013). Our findings from mantle peridotite samples are consistent with those of FAB studies.

Our best fit models showed that the Tonga samples can be reproduced by models with the DMM, whereas the IBM samples can be reproduced by models using either the DMM or the DDMM (Figs. 4, S-8). Accumulated melts in the IBM best fit models are slightly more LREE enriched when derived from the DMM compared to the DDMM, as reflected in the modal Ce contents (Fig. S-7). Studies on FAB have also suggested a source depleted by ~0.5–2 % relative to the DMM (Umino *et al.*, 2018; Yogodzinski *et al.*, 2018; Shervais *et al.*, 2019). This degree of prior depletion is consistent with the difference between the DMM and DDMM sources (Workman and Hart, 2005). Therefore, a source more depleted than the DMM, such as the DDMM may be more consistent with the IBM samples. The compiled forearc spinel data set shows that Cr# above 0.8 occur in the IBM, but not in the Tonga (Fig. 1), in agreement with the higher best fit F in the IBM (16.8 %) compared to the Tonga (7.4 %). Although further study is necessary, our model results and spinel Cr# systematics indicate potential regional variability, in agreement with studies of early basalts (Arculus *et al.*, 2019), which potentially reflect differences such as the subduction initiation style and source mantle composition.

Conclusions

We examined the least depleted harzburgites from the IBM forearc and a lherzolite from the Tonga forearc among the rare ~4 % population among forearc peridotites. They show low spinel Cr#, and LREE depleted patterns in clinopyroxenes and amphiboles. These characteristics differ from the typical depleted forearc peridotites after boninitic magma extraction. Our open system melting models reproduced the REE contents of the studied clinopyroxenes and early basalts, and amphiboles of each region. We identified the IBM and Tonga peridotites as residual peridotites after the extraction of early basaltic magma during subduction initiation. The LREE depleted patterns of clinopyroxenes and amphiboles suggest that the IBM and Tonga peridotites may have formed through near fractional melting under moist conditions. These forearc peridotites are very rare, but essential to understand the controlling factors of subduction initiation such as source mantle compositions and style of subduction initiation style.

Data Availability

All data and Supplementary Information are available in online.

Acknowledgments

We thank P. Waterton and K. Ozawa for their help with the modelling and best fit estimation, and T. Mizukami, and Y. Ichiyama for discussions, and H. Yamashita for providing the samples. We thank J. Pearce, K.Y. Lin, and J. Hermann for reviews of a previous version of this manuscript. We thank V. Basch, an anonymous reviewer, and Editor R.O.C. Fonseca for their constructive comments, which improved the paper.

Editor: Raul O.C. Fonseca

Funding

This study was supported by Japan Society for the Promotion of Science (no. 24JK0076 and no. 23K25963).

Declaration of Competing Interest

The authors declare that they have no known competing financial interests or personal relationships that could have appeared to influence the work reported in this paper.

Additional Information

Supplementary Information accompanies this letter at https://www.geochemicalperspectivesletters.org/article2624.

Cite this letter as: Nishio, I., Akizawa, N., Ishii, T., Itano, K., Tamura, A., Morishita, T. (2026) Residual forearc peridotites recording the early magmatic stage of subduction initiation. *Geochem. Persp. Let.* 41, 1–6. https://doi.org/10.7185/geochemlet.2624

References

Akizawa, N., Ohara, Y., Okino, K., Ishizuka, O., Yamashita, H., Machida, S., Sanfilippo, A., Basch, V., Snow, J.E., Sen, A., Hirauchi, K.-i., Michibayashi, K., Harigane, Y., Fujii, M., Asanuma, H., Hirata, T. (2021) Geochemical characteristics of back-arc basin lower crust and upper mantle at final spreading stage of Shikoku Basin: an example of Mado Megamullion. *Progress in Earth and Planetary Science* 8, 65. https://doi.org/10.1186/s40645-021-00454-3

Arculus, R.J., Gurnis, M., Ishizuka, O., Reagan, M.K., Pearce, J.A., Sutherland, R. (2019) How to create new subduction zones: A global perspective. *Oceanography* 32, 160–174. https://doi.org/10.5670/oceanog.2019.140

Birner, S.K., Warren, J.M., Cottrell, E., Davis, F.A., Kelley, K.A., Falloon, T.J. (2017) Forearc Peridotites from Tonga Record Heterogeneous Oxidation of the Mantle following Subduction Initiation. *Journal of Petrology* 58, 1755–1780. https://doi.org/10.1093/petrology/egx072

Brounce, M., Reagan, M.K., Kelley, K.A., Cottrell, E., Shimizu, K., Almeev, R. (2021) Covariation of Slab Tracers, Volatiles, and Oxidation During Subduction Initiation. *Geochemistry, Geophysics, Geosystems* 22, e2021GC009823. https://doi.org/10.1029/2021GC009823

Cipriani, A., Bonatti, E., Seyler, M., Brueckner, H.K., Brunelli, D., Dallai, L., Hemming, S.R., Ligi, M., Ottolini, L., Turrin, B.D. (2009) A 19 to 17 Ma amagmatic extension event at the Mid-Atlantic Ridge: Ultramafic mylonites from the Vema Lithospheric Section. *Geochemistry, Geophysics, Geosystems* 10, Q10011. https://doi.org/10.1029/2009GC002534

Crameri, F., Magni, V., Domeier, M., Shephard, G.E., Chotalia, K., Cooper, G., Eakin, C.M., Grima, A.G., Gürer, D., Király, Á., Mulyukova, E., Peters, K., Robert, B., Thielmann, M. (2020) A transdisciplinary and community-driven database to unravel subduction zone initiation. *Nature Communications* 11, 3750. https://doi.org/10.1038/s41467-020-17522-9

Day, J.M.D., Brown, D.B. (2021) Ancient Melt-Depletion in Fresh to Strongly Serpentinized Tonga Trench Peridotites. *Journal of Petrology* 62, egab088. https://doi.org/10.1093/petrology/egab088

Gong, X., Tian, L., Dong, Y. (2022) Contrasting melt percolation and melt-rock reactions in the Parece Vela back-arc oceanic lithosphere, Philippine Sea: A mineralogical perspective. *Lithos* 422–423, 106727. https://doi.org/10.1016/j.lithos.2022.106727

Ichiyama, Y., Tsujimori, T., Fryer, P., Michibayashi, K., Tamura, A., Morishita, T. (2021) Temporal and spatial mineralogical changes in clasts from Mariana serpentinite mud volcanoes: Cooling of the hot forearc-mantle at subduction initiation. *Lithos* 384–385, 105941. https://doi.org/10.1016/j.lithos.2020.105941

Ishii, T., Robinson, P.T., Maekawa, H., Fiske, R. (1992) Petrological studies of peridotites from diapiric serpentinite seamounts in the Izu-Ogasawara-Mariana Forearc, Leg 125. In: Fryer, P., Pearce, J.A., Stokking, L.B., Ali, J.R., Arculus, R., *et al.* (Eds.) *Proceedings of the Ocean Drilling Program, Scientific Results,* 125, Ocean Drilling Program, College Station, TX, 445–485. https://doi.org/10.2973/odp.proc.sr.125.129.1992

Ishizuka, O., Tani, K., Reagan, M.K., Kanayama, K., Umino, S., Harigane, Y., Sakamoto, I., Miyajima, Y., Yuasa, M., Dunkley, D.J. (2011) The timescales of subduction initiation and subsequent evolution of an oceanic island arc. *Earth and Planetary Science Letters* 306, 229–240. https://doi.org/10.1016/j.epsl.2011.04.006

Ishizuka, O., Taylor, R.N., Umino, S., Kanayama, K. (2020) Geochemical Evolution of Arc and Slab Following Subduction Initiation: a Record from the Bonin Islands, Japan. *Journal of Petrology* 61, egaa050. https://doi.org/10.1093/petrology/egaa050

Li, Y.-B., Kimura, J.-I., Machida, S., Ishii, T., Ishiwatari, A., Maruyama, S., Qiu, H.-N., Ishikawa, T., Kato, Y., Haraguchi, S., Takahata, N., Hirahara, Y., Miyazaki, T. (2013) High-Mg Adakite and Low-Ca Boninite from a Bonin Fore-arc Seamount: Implications for the Reaction between Slab Melts and Depleted Mantle. *Journal of Petrology* 54, 1149–1175. https://doi.org/10.1093/petrology/egt008

Loocke, M.P., Snow, J.E. (2024) Arc Foundations and Subduction Initiation: Insights into the Magmatic Evolution of the Lower Crust/Upper Mantle of the Izu–Bonin Forearc during Subduction Initiation. *Journal of Petrology* 65, egae038. https://doi.org/10.1093/petrology/egae038

MacLeod, C.J., Lissenberg, C.J., Bibby, L.E. (2013) “Moist MORB” axial magmatism in the Oman ophiolite: The evidence against a mid-ocean ridge origin. *Geology* 41, 459–462. https://doi.org/10.1130/G33904.1

Maunder, B., Prytulak, J., Goes, S., Reagan, M. (2020) Rapid subduction initiation and magmatism in the Western Pacific driven by internal vertical forces. *Nature Communications* 11, 1874. https://doi.org/10.1038/s41467-020-15737-4

Meffre, S., Falloon, T.J., Crawford, T.J., Hoernle, K., Hauff, F., Duncan, R.A., Bloomer, S.H., Wright, D.J. (2012) Basalts erupted along the Tongan fore arc during subduction initiation: Evidence from geochronology of dredged rocks from the Tonga fore arc and trench. *Geochemistry, Geophysics, Geosystems* 13, Q12003. https://doi.org/10.1029/2012GC004335

Morishita, T., Tani, K., Shukuno, H., Harigane, Y., Tamura, A., Kumagai, H., Hellebrand, E. (2011) Diversity of melt conduits in the Izu-Bonin-Mariana forearc mantle: Implications for the earliest stage of arc magmatism. *Geology* 39, 411–414. https://doi.org/10.1130/G31706.1

Nishio, I., Morishita, T., Tamura, A., Itano, K., Takamizawa, S., Ichiyama, Y., Arai, S., Barrett, N., Szilas, K. (2023) Formation of Ultra-Depleted Mantle Peridotites and Their Relationship With Boninitic Melts: An Example From the Kamuikotan Unit, Hokkaido, Japan. *Journal of Geophysical Research: Solid Earth* 128, e2022JB025066. https://doi.org/10.1029/2022JB025066

Ozawa, K. (2001) Mass balance equations for open magmatic systems: Trace element behavior and its application to open system melting in the upper mantle. *Journal of Geophysical Research: Solid Earth* 106, 13407–13434. https://doi.org/10.1029/2001JB900001

Pearce, J.A., Barker, P.F., Edwards, S.J., Parkinson, I.J., Leat, P.T. (2000) Geochemistry and tectonic significance of peridotites from the South Sandwich arc–basin system, South Atlantic. *Contributions to Mineralogy and Petrology* 139, 36–53. https://doi.org/10.1007/s004100050572

Prigent, C., Agard, P., Guillot, S., Godard, M., Dubacq, B. (2018) Mantle Wedge (De)formation During Subduction Infancy: Evidence from the Base of the Semail Ophiolitic Mantle. *Journal of Petrology* 59, 2061–2092. https://doi.org/10.1093/petrology/egy090

Reagan, M.K., Ishizuka, O., Stern, R.J., Kelley, K.A., Ohara, Y., Blichert-Toft, J., Bloomer, S.H., Cash, J., Fryer, P., Hanan, B.B., Hickey-Vargas, R., Ishii, T., Kimura, J.-I., Peate, D.W., Rowe, M.C., Woods, M. (2010) Fore-arc basalts and subduction initiation in the Izu-Bonin-Mariana system. *Geochemistry, Geophysics, Geosystems* 11, Q03X12. https://doi.org/10.1029/2009GC002871

Shervais, J.W., Reagan, M., Haugen, E., Almeev, R.R., Pearce, J.A., Prytulak, J., Ryan, J.G., Whattam, S.A., Godard, M., Chapman, T., Li, H., Kurz, W., Nelson, W.R., Heaton, D., Kirchenbaur, M., Shimizu, K., Sakuyama, T., Li, Y., Vetter, S.K. (2019) Magmatic Response to Subduction Initiation: Part 1. Fore-arc Basalts of the Izu-Bonin Arc From IODP Expedition 352. *Geochemistry, Geophysics, Geosystems* 20, 314–338. https://doi.org/10.1029/2018GC007731

Stern, R.J., Gerya, T. (2018) Subduction initiation in nature and models: A review. *Tectonophysics* 746, 173–198. https://doi.org/10.1016/j.tecto.2017.10.014

Todd, E., Gill, J.B., Pearce, J.A. (2012) A variably enriched mantle wedge and contrasting melt types during arc stages following subduction initiation in Fiji and Tonga, southwest Pacific. *Earth and Planetary Science Letters* 335–336, 180–194. https://doi.org/10.1016/j.epsl.2012.05.006

Umino, S., Kanayama, K., Kitamura, K., Tamura, A., Ishizuka, O., Senda, R., Arai, S. (2018) Did boninite originate from the heterogeneous mantle with recycled ancient slab? *Island Arc* 27, e12221. https://doi.org/10.1111/iar.12221

Warren, J.M. (2016) Global variations in abyssal peridotite compositions. *Lithos* 248–251, 193–219. https://doi.org/10.1016/j.lithos.2015.12.023

Workman, R.K., Hart, S.R. (2005) Major and trace element composition of the depleted MORB mantle (DMM). *Earth and Planetary Science Letters* 231, 53–72. https://doi.org/10.1016/j.epsl.2004.12.005

Yogodzinski, G.M., Bizimis, M., Hickey-Vargas, R., McCarthy, A., Hocking, B.D., Savov, I.P., Ishizuka, O., Arculus, R. (2018) Implications of Eocene-age Philippine Sea and forearc basalts for initiation and early history of the Izu-Bonin-Mariana arc. *Geochimica et Cosmochimica Acta* 228, 136–156. https://doi.org/10.1016/j.gca.2018.02.047